Journal of Atmospheric and Solar–Terrestrial Physics 240 (2022) 105963

Contents lists available at ScienceDirect

Journal of Atmospheric and Solar-Terrestrial Physics

journal homepage: www.elsevier.com/locate/jastp

Research Paper

Patterns of geomagnetic Pc1 pulsations in different solar cycles in the near-equatorial region from the Indian subcontinent

Jayashree Bulusu [a], Vyacheslav Pilipenko [b], Kusumita Arora [c,*], C. Prasanna Simha [d,e]

[a] Indian Institute of Geomagnetism, Navi Mumbai, India
[b] Institute of Physics of the Earth, Moscow, Russia
[c] CSIR-National Geophysical Research Institute, Hyderabad, Telangana, India
[d] Institute of Seismological Research, Gandhi Nagar, Gujarat, India
[e] M. G. Science Institute, Gujarat University, Ahmedabad, Gujarat, India

ARTICLE INFO

Keywords:
Pc1 pulsations
Low-latitude investigation
Solar cycle dependence
Seasonal variation
Geomagnetic storm

ABSTRACT

Pc1 geomagnetic pulsations have been investigated at very low latitudes using 13 years of archived records covering solar cycle 20–21 from the equatorial site Choutuppal (CPL, L = 1.03), and 5 years of digital induction coil magnetometer data covering descending phase of solar cycle 24 from the low latitude site Desalpar (DSP, L = 1.07). At CPL, the maximum number of Pc1 events is seen in the declining phase of the solar cycle 20 and minimum occurrence is observed in the ascending phase of the solar cycle 21. In contrast, at DSP, the Pc1 occurrence shows a maximum during solar maximum and a minimum in the declining phase of solar cycle 24. The annual and seasonal patterns of Pc1 occurrence show an inverse relation with sunspot numbers at both stations. The seasonal variation of Pc1 occurrence has a maximum in December solstice at CPL and in June solstice at DSP, respectively. The diurnal variations of Pc1 activity show similar trends at both locations with maximum Pc1 occurrence during pre- and post-midnight sectors. The superposed epoch analysis shows minimum number of Pc1s in the initial phase, followed by Pc1 occurrence in the main phase, increasing significantly in the recovery phase of geomagnetic storms. The role of ionospheric plasma density and attenuation of Pc1 waves upon propagation via the ionospheric waveguide is presented.

1. Introduction

Electromagnetic ion cyclotron (EMIC) waves in the Pc1 frequency band (from 0.1 Hz to several Hz), generated by resonant wave-particle interactions, are an important component of space weather in the near-Earth environment. These waves may cause depletion of MeV-electron fluxes in the outer radiation belt (Shprits et al., 2016; Usanova et al., 2014), limit the lifetime of energetic ring current protons (Kennel and Petchek, 1966), and produce localized proton aurora (Yahnin et al., 2007). Even a relatively weak injection of ring current protons into the inner magnetosphere or solar wind pressure pulses can stimulate the onset of the EMIC instability, when the energetic component of the magnetospheric plasma is near the marginal state. Once generated near the equatorial plane of the magnetosphere, EMIC waves propagate along magnetic field lines, transverse the ionosphere, and finally reach the ground. The primary source regions of Pc1 generation is around the plasmapause, where the temperature anisotropy is achieved upon injection of the energetic ions into the dense cold plasma, and the dayside boundary regions of the magnetosphere (Pickett et al., 2010).

Within the ionosphere, an EMIC wave is partially converted to an ionospheric waveguide mode that can be carried thousands of km relative to the locations of the wave injection (Kuwashima et al., 1981; Kim et al., 2011; Fraser et al., 2006). The horizontal ducted propagation is not isotropic, but most efficient along the magnetic meridian (Greifinger, 1973). Thus, the ionosphere operates as an enormous "receiving antenna" collecting magnetospheric EMIC signals from a large area around a ground observer. Pc1 waves propagating from an injection region along the ionosphere are found to decrease their intensity in a specific way: the attenuation is very rapid (~10 dB/100 km) in the injection center, but become much weak (~2.5 dB/100 km) in the region beyond ~500 km (Hayashi et al., 1981; Kim et al., 2010).

The intensity and occurrence rate of Pc1 waves on the ground are determined by three processes: generation in the near-equatorial plane, propagation through the magnetospheric plasma from the top of the

* Corresponding author.
E-mail addresses: karora@ngri.res.in, karora.ngri@yahoo.co.uk (K. Arora).

https://doi.org/10.1016/j.jastp.2022.105963
Received 27 December 2021; Received in revised form 12 September 2022; Accepted 29 September 2022
Available online 4 October 2022

field line to the upper ionosphere, and eventually transmission through the ionosphere to the ground. Subsequent to field-aligned propagation in a multi-ion magnetospheric plasma, Pc1 waves may encounter the cross-over region where wave mode partial absorption/conversion/reflection occurs (Lee et al., 2008). All these processes depend on many space weather parameters. It is not yet established whether the relative contributions of the generation/propagation processes in the magnetosphere and ionosphere to the Pc1 activity on the ground differ at different latitudes. Most frequently Pc1 waves appear at middle latitudes (Posch et al., 2010) and in the subauroral region (Fraser et al., 1996), although there have been evidences of Pc1 pulsation that appear over open geomagnetic field line like the cusp region (Engebretson et al., 2009), plasma mantle (Engebretson et al., 2012), and the polar cap (Pilipenko et al., 2011).

All the studies listed above have been performed at high and middle latitudes. Investigations on the low and equatorial regions have received less attention. In a recent study, Kim et al. (2020) statistically analyzed Pc1 pulsations observed by a Bohyunsan (BOH) magneto-impedance sensor located in Korea (L = 1.3) for solar cycle 24 and in the ascending phase of solar cycle 25. It was shown that at these latitudes the Pc1 waves frequently occurred in March in the dawn (1–3 MLT) sector, during the declining phase of the solar cycle. Pc1 occurrence was reported to be strongly dependent on geomagnetic conditions, and was especially high during the recovery phase of the geomagnetic storm. Using data from Low Earth Orbiting (LEO) satellites, Park et al. (2013) demonstrated the hemispherical asymmetry in the occurrence pattern of Pc1s during June and December Solstice. The number of occurrences was larger during June solstices in the northern hemisphere, while this asymmetry was insignificant in the southern hemisphere. Webster and Fraser (1984, 1985) showed that Pc1 pulsations observed at two stations at L = 1.9 have source inside plasmapause region, lasting from a few minutes to half an hour and fall in the lower frequency range (0.5 Hz–2.1 Hz). Pc1 pulsations at high latitudes were most frequently observed during the daytime, but at low latitudes the occurrence maximum was always in the nighttime (Kuwashima et al., 1981; Nomura et al., 2011). At low latitudes (L∼1.1) higher frequency Pc1 (∼4.5 mHz) were reported from Indian region (Sinha et al., 2007). The number of Pc1s were higher during the post sunset and predawn hours. Nine years of archived data from Choutuppal (L = 1.03) during 1965–1974 were investigated and the periods of pearls were seen to be influenced by the average magnetic activity level prevailing preceding few days prior to the active day (Sastry et al., 1978).

Long geomagnetic records are essential for understanding the Pc1 characteristics during phases of the solar cycle. Mursula et al. (1991) analyzed the magnetograms of the high latitude station of Sodankylä (SOD, 67°22′ GGlat, 26°38’ GGlong, 63.9° CGMlat) over the whole registration period covering nearly four solar cycles. The results show a very strong negative correlation between the annual Pc1 activity and the annual sunspot number. Kangas et al. (1998) and Guglielmi et al. (2006) found an anticorrelation between the ground Pc1 occurrence and solar activity. The Pc1 statistics from CHAMP satellite showed a dominance of activity in the upper ionosphere during solar minimum years (Park et al., 2013).

Higher Pc1 activity from ground data during solar minimum years was attributed to an enhanced wave reflection from the ionosphere during these periods, and, consequently, more efficient operation of the magnetospheric wave-bounce master (Trakhtengerts et al., 2000). This long stated inverse relation of the Pc1 occurrence with solar cycle is now countered from more recent studies, showing minimum number of Pc1s occurring during the quietest year 2009 of solar cycle 23 (Anisimov et al., 2018). Enhanced absorption in the solar illuminated ionosphere can also contribute to a lower level of Pc1 activity during solar maxima years. Also, during the period of solar maximum the transmission rate of Pc1 waves to the ground may be worse than during the solar minimum. The low amplitude of Pc1 at low latitude stations during day time was attributed to the enhanced attenuation of waves during duct propagation in the ionosphere from high to low latitudes (Greifinger and Greifinger, 1973; Kuwashima et al., 1981).

In the present study, the differences in the properties of Pc1s are tested in different solar cycles using data for a period of 1970–1983 based on unique digitized archive and digital data during 2013–2018 from the same region to elucidate the similarities and distinct differences of Pc1 characteristics during different seasons and different phases of solar cycles.

2. Observational data

This study uses two type of data records:

(a) Digital records during 2013–2018 (latter part of solar cycle 24) of induction coil magnetometer with 64 Hz sampling frequency from Desalpar (DSP) station with coordinates L = 1.08, geographic latitude 23.7425 N and longitude 70.6464 E, and geomagnetic latitude 18.31 N and longitude 143.84 E (Computed based on the DGRF/IGRF geomagnetic field models for Epochs, 1900–2025), local time LT = UT+0530;

(b) archived paper-chart records for the period 1970–1983 (descending phase of solar cycle 20 and ascending phase of 21) from Choutuppal (CPL) station about 60 km east of Hyderabad with coordinates L = 1.03, geographic 17.41 N and 78.55 E, and geomagnetic 7.64 N and 150.5 E), local time (UT+0530).

The period of investigation at these two sites are different, which provides an opportunity to compare the statistical characteristics of Pc1 activity at very low latitudes during different solar cycles. CPL is the near-equatorial station (Fig. 1). Though the dip equator has migrated further south of the Indian subcontinent at the present epoch 2015 (blue curve in Fig. 1), in both time intervals DSP falls into the low latitude region.

The induction coil magnetometer at DSP measures variations of geomagnetic north-south (X), east-west (Y), and vertical (Z) components. The operating range of frequency is 0.001–30 Hz. The data of each day were checked for noise and outliers were removed. The de-noised and de-spiked data were analyzed using time-frequency analysis for identification of dominant spectral peak. The analysis is performed by constructing a spectrogram of the down-sampled data to 8 Hz in a running time window of 256 data points (interval of ∼22 min), applying a Hamming window, and subjecting it to Fourier transform. Each subsequent window was shifted by 56 points (∼5 min), thereby allowing an overlap of 200 data points (∼17 min). The frequency resolution for the dynamic spectra is 0.03 Hz. Only those events in the frequency range of 0.2–5 Hz were considered which lasted at least for 5-min. A total of 208 events were identified in the X component out of which 203 events were also seen in the Y component during 2013–2018. It should be noted that ICM data from this station was available continuously from June 2013 to December 2015. For later years, the availability of data was not continuous and could be included for our investigation for specific intervals of data (refer Fig. A1 in Appendix for availability of data at DSP).

Analogue paper-chart records were obtained from three component induction coil magnetometer at CPL during 1969–1990 by CSIR-NGRI (Sarma et al., 1969). The recording system was of induction type having high permeability core-coil sensor, with a feedback arrangement to facilitate recording of actual variation in the field rather than the rate of change. Three identical coils were placed in the geomagnetic north-south, east-west and vertical directions for recording pulsations in the X, Y and Z components. The magnetic fields were recorded at an Ultra-Quick-Run chart speed of 30 mm/min for measuring pulsations with periods less than 20 s (Sastry et al., 1983). Metadata from archived records are tabulated in different period bins and the Pc1 signatures are identified. A total of 649 Pc1 events are retrieved for the duration 1971–1983. Complete details of data availability from CPL is shown in bottom panel of Fig. A1 in Appendix section.

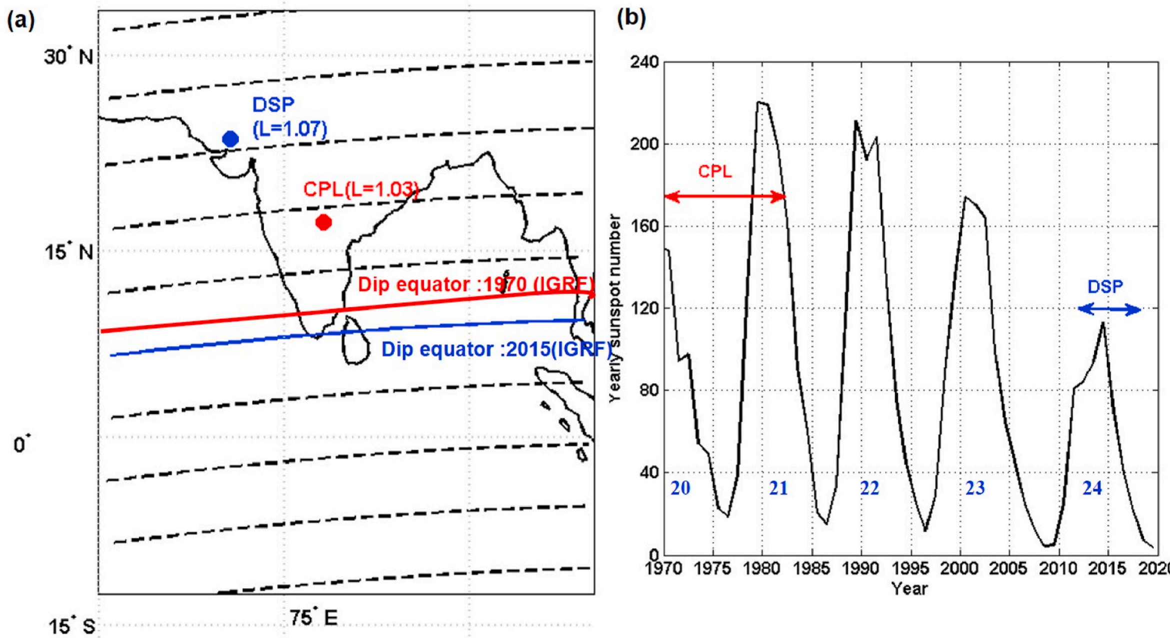

Fig. 1. (a) Location of ground magnetic stations used in the present investigation. Position of dip equators as computed using IGRF model for epoch 1970 and 2015 marked as black and red curve. (b) Solar cycle variation superimposed with the availability of geomagnetic data at CPL and DSP respectively.

3. Examples of typical Pc1 pulsations at low and equatorial latitudes

We initially present typical Pc1 events seen during quiet and disturbed geomagnetic conditions at low-latitude DSP station.

3.1. Quiet time Pc1 pulsation at DSP on March 25, 2013

This event occurred during early morning hours 2154–2300 UT on March 25, 2013 on the geomagnetically quiet background: solar wind speed 395 km/s, Dst −16 nT, planetary Kp index 1.67, SYM-H index ∼ −10 nT. Two bursts of Pc1s are evident in spectrogram with duration of ∼15 min each. The spectrogram shows a narrowband emission in both X and Y components (Fig. 2a and b) with a peak frequency of 1.5 Hz. The spectral power in X component is nearly the same as in Y component (Fig. 2c).

3.2. Disturbed time Pc1 pulsation on DSP on March 17, 2013

A long lasting Pc1 signature is observed during 1200–1630 UT on March 17, 2013. After 1600 UT the central frequency gradually increases in both X and Y components (Fig. 3a and b). The spectral peak

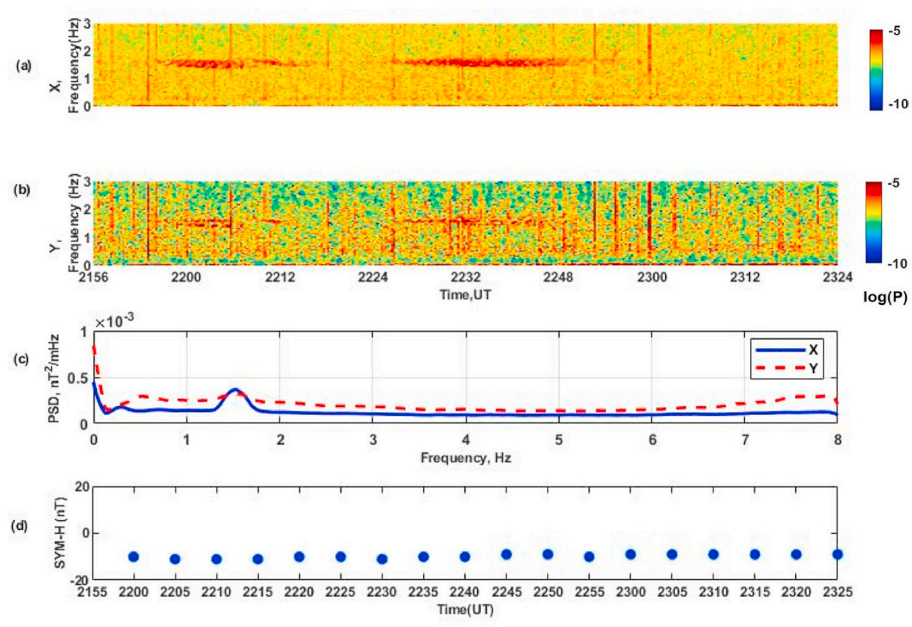

Fig. 2. Quiet time signature of Pc1 geomagnetic pulsation recorded at DSP during 2154–2300 UT in X (a) and Y (b) components on March 25, 2013. Panels (a,b) show spectrograms of induction magnetometer record, panel (c) presents the power spectral estimation of the observed event, panel (d) shows the equatorial SYM-H index.

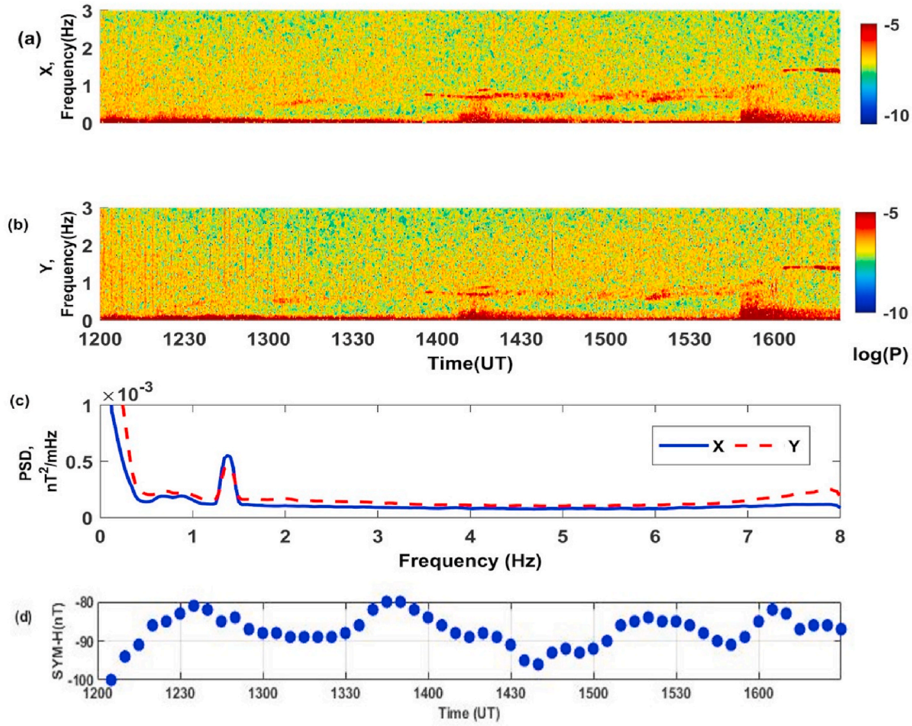

Fig. 3. Panels have their similar format as in Fig. 2 representing the disturbed time Pc1 which occurred during the recovery phase of an intense geomagnetic storm on March 17, 2013.

frequency is 1.40 Hz, the spectral power is 1.2 times higher in X component as compared to Y component (Fig. 3c). Event was observed as the geomagnetic storm progressed from main to recovery phase with SYM-H index changing from −100 nT, to −80 nT (Fig. 3d).

3.3. Multi-band Pc1 pulsations at DSP on January 09, 2015

This event shows a rare example of multi-band Pc1 event which lasted for 2 h in the dawn sector (00–0230 UT (LT=UT+0530)) on January 09, 2015 (Fig. 4). Initially a constant frequency of 3 Hz is observed for an hour that ended as multi-harmonic frequencies during 0200–0230 UT in the X component with the fundamental frequency of 0.8 Hz. The geomagnetic background was quiet with Dst varying between −35 nT and −45 nT. The amplitude in Y component is higher than X component for this particular event. It should be noted that only 3 of total 203 events showcase such multiband oscillations in Pc1. These

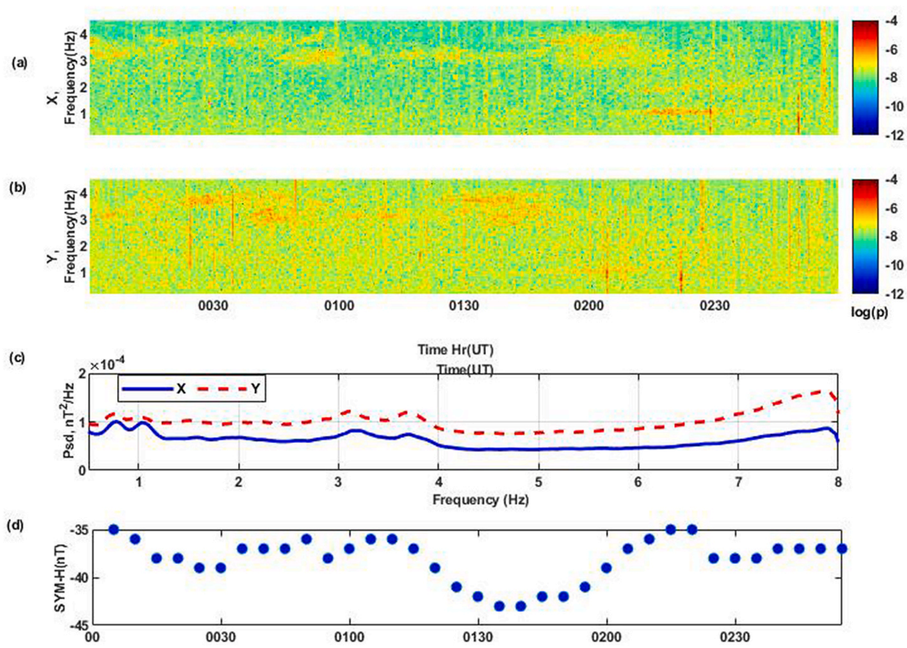

Fig. 4. Panels have their similar format as in Fig. 2 representing the multi-band Pc1 structure Same as Fig. 2 during the recovery phase of a moderate storm, on January 09, 2015.

events are excluded from the statistical analysis.

Fig. 5 shows the analogue ultra-quick run charts recorded at the equatorial station CPL, that represents the noon time Pc1 oscillation on August 28, 1981 during 0526–0536 UT and 0745–0749 UT. The analogue charts were scaled and tabulated to obtain the frequency of the Pc1 event as described in Bulusu et al., 2017. Data from photographic charts were manually recorded using a graph that could provide the period of pulsations in different frequency range. The obtained periods of pulsations were included in a tabular format providing the details of the pulsation observed. For example, the type of pulsation, period of pulsation, beginning and ending of pulsation event. In this way, volume of metadata archived was created that spread over 14 years (1971–1984) for CPL observatory. This data was published in different volumes quarterly by the CSIR-NGRI.

From top to bottom two horizontal traces represent the hourly variation in the short periods (<5 s) of the geomagnetic field (Fig. 5). Two consecutive bursts seen with frequencies of 0.5 Hz and 0.3 Hz respectively can be seen.

4. Statistical properties of Pc1 events at low latitude (DSP station)

4.1. Diurnal patterns

The diurnal occurrence pattern shows that maximum number of Pc1s occur in the pre-midnight hours (2200–2400 LT) followed by a secondary peak in post-midnight hours (0400–0600 LT) (Fig. 6a). Minimum number of Pc1 are seen around local noon.

The local time variation of frequency of Pc1 shows that most of the high-frequency Pc1 events (>1.5 Hz) are seen during local noon (Fig. 6b), and only few events in this frequency range occur in post-midnight and pre-midnight sectors. On contrary, only one low-frequency Pc1 event (<1 Hz) is seen during local noon.

4.2. Seasonal patterns

Seasonal variations are estimated using Pc1 events which occurred in different seasons: June solstices (covers events from months May–August), December Solstices (events from November–February) and Equinox consists of March, April, September and October for each year presented in Fig. 6. Maximum of Pc1 occurrence is seen at June solstice, whereas minimum number of Pc1 events are seen during equinox (Fig. 6c).

To highlight the distinction between different frequency bands of Pc1s, all recorded events were grouped to three bins of 0.2–1 Hz, 1–2 Hz, and >2 Hz. About 85% of Pc1s fall in the low-frequency bin 0.2–1 Hz bin, whereas 9% events are in the bin 1–2 Hz (Fig. 7a). Only 6% of events fall in the highest-frequency bin >2 Hz. Corresponding histogram for all Pc1events, which includes finer bins of frequency distribution is shown in Fig. 7b, indicates 0.2 Hz as the dominant peak. The distribution of higher frequency events is not monotonic, but specific range of frequencies are highlighted.

5. Statistical properties of Pc1 events at near-equatorial region (CPL station)

5.1. Diurnal pattern

The diurnal occurrence pattern of Pc1s shows a peak in the post-midnight sector (0200–0400 LT), followed by a secondary maximum in the pre-midnight sector with almost half the occurrence rate (Fig. 8a). Pc1 occurrence is significantly lower during near-noon hours. Pc1 frequencies show a random occurrence pattern with local time (Fig. 8b).

5.2. Seasonal pattern

The seasonal patterns show that Pc1 occurrence shows a peak in December solstices and a minimum during June solstice (Fig. 8c). Fig. 9 shows that around 56% of events populate the frequency band of 1–2 Hz, followed by 30% events within 2–3 Hz frequency range at CPL. Only 14% events fall in frequency range if 0.2–1 Hz (Fig. 9a). Corresponding histogram for all Pc1events indicate 1.5 Hz as the dominant peak frequency (Fig. 9b).

6. .Relation of Pc1 occurrence at low and equatorial latitudes with geomagnetic storms

For elucidating the relationship between the Pc1 geomagnetic pulsations with geomagnetic storms, we apply the superposed epoch analysis to relate the Pc1 occurrence with geomagnetic storms with $|Dst|>$ 50 nT. Day 0 marks the main phase of storm with maximum depression in the Dst index and all Pc1 events within 4 h of maximum depression are considered to be associated with the main phase of the storm. Day 1 marks the beginning of the recovery phase and subsequent days of recovery phase are determined in 24 h interval as Day 2, Day 3 and so on. Thus, Days −4 to −1 represent storm phase's quiet and initial phase of the geomagnetic storm. Day −1 denotes the Storm Sudden Commencement (SSC) phase. Day 0 marks main phase of the storm. Days 1–6 marks the early and late recovery phase of the geomagnetic storm. The number of Pc1 events are classified accordingly to different phases and the result are shown in Fig. 10.

Based on the above-mentioned conditions, a total of 156 events and 306 events are selected at DSP and CPL respectively. A comparison between the two low latitude sites indicate that around 11% and 14% of Pc1 events occur during the initial phase at DSP and CPL respectively. In the main phase of the geomagnetic storms (marked as Day 0), 36 Pc1 events occur at DSP and 62 events occur at CPL. In the early recovery phase of the geomagnetic storm (Day 1 and Day 2), a total of 42 and 76 Pc1 events are seen at DSP and CPL respectively. In the late recovery phase (Day 3-Day 7), a total of 48 and 71 events occur at DSP and CPL. The number of Pc1 events during the main phase of the storm shows a peak at both the stations. However, it should be noted that the total number of Pc1 events observed in the recovery phase (lasting over 4–6 days) are more in number at both the sites. Thus, more than 50% of observed Pc1s are seen to occur in the recovery phase similar to the results of Bortnik et al., 2008. In the main phase, 23% and 20% of Pc1 events at DSP and CPL respectively. Around 48% and 53% events are

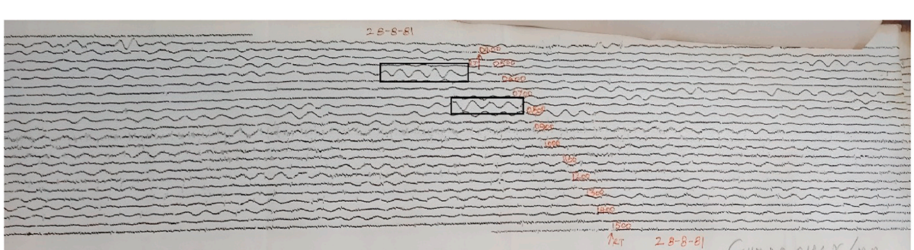

Fig. 5. Typical analogue records with Ultra-quick run setup on August 28, 1981, 0526–0535 UT and 0745–0749 UT.

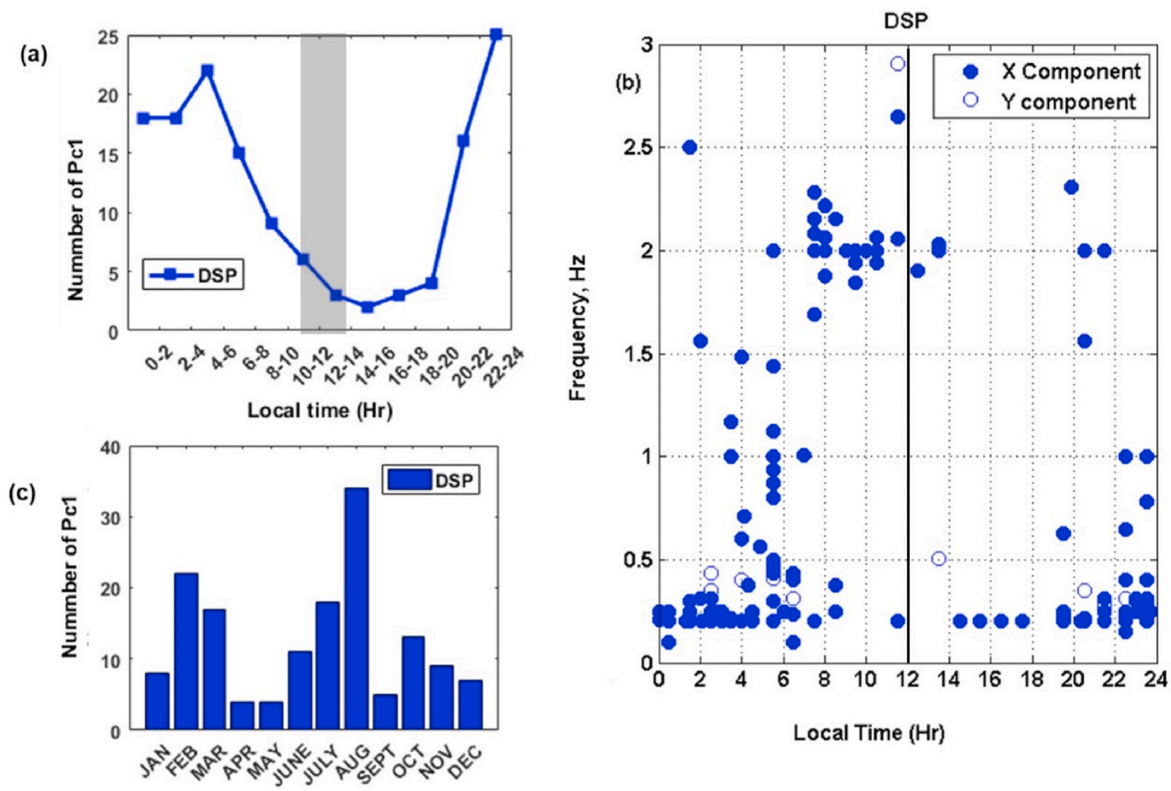

Fig. 6. Diurnal variation of (a) occurrence and (b) frequency distribution of Pc1 events at low-latitude DSP station. Seasonal variation of Pc1 occurrence is shown in panel (c). The shaded area in panel (a) and vertical line in panel (b) mark the local noon at DSP.

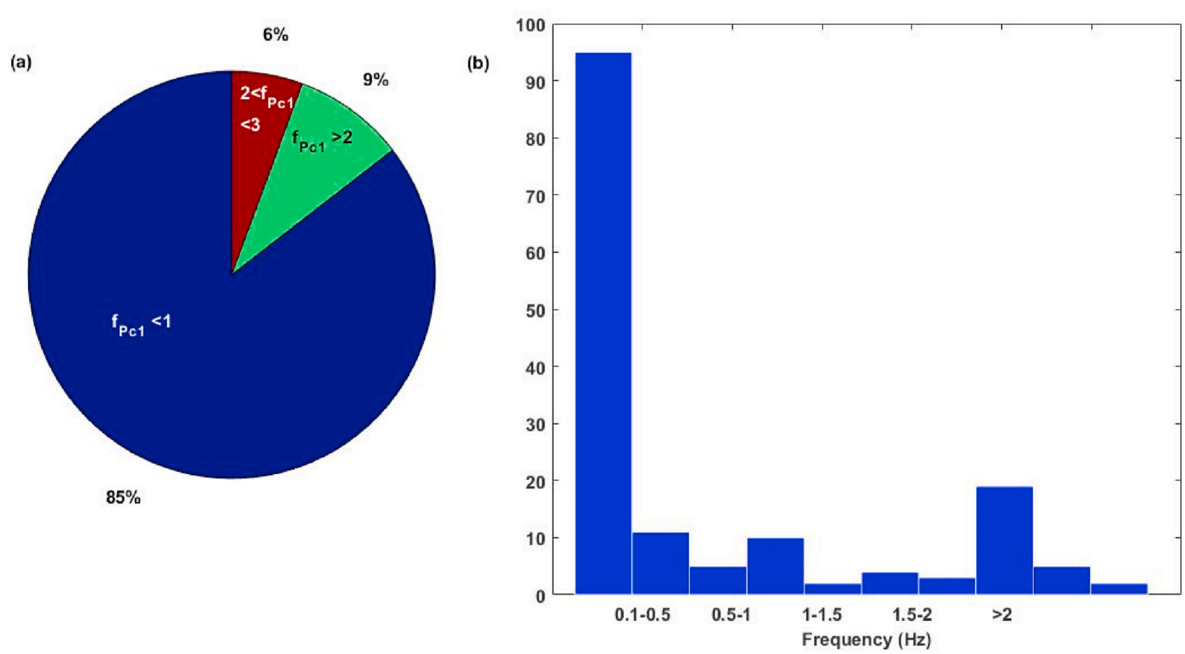

Fig. 7. Frequency distribution of Pc1 events recorded at DSP: (a) pie chart showing the occurrence in different bins and (b) histogram to indicate the dominant peak.

seen in the early and late recovery phase at DSP and CPL respectively.

A typical example of Pc1 occurrence around an intense storm is shown in Fig. 10b. The storm was initiated on March 17, 2015 and reached to the maximum depression of −227 nT at around 0700 UT on March 17, 2015. The variation of Dst index is shown in the left ordinate. The right ordinate of panel 10 b marks the number of Pc1s that were observed in the recovery phase of the storm. Around 6 PC1s were observed during the recovery phase during dusk-midnight sector.

7. Solar cycle dependence

Hourly values of sunspot number R, activity indices are obtained from CDAweb (https://cdaweb.gsfc.nasa.gov). There was a significant change in the solar cycle variation in terms of amplitude and length of

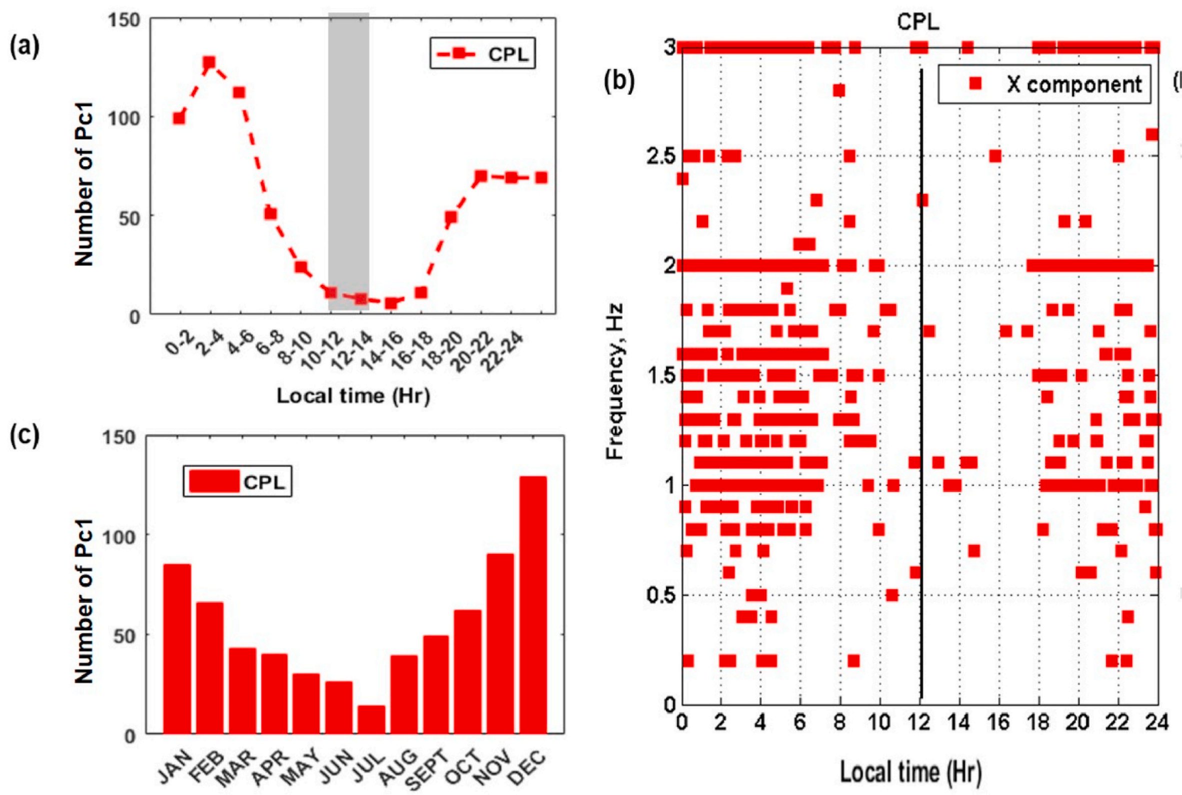

Fig. 8. Same as Fig. 6, but for CPL station during 1970–1983.

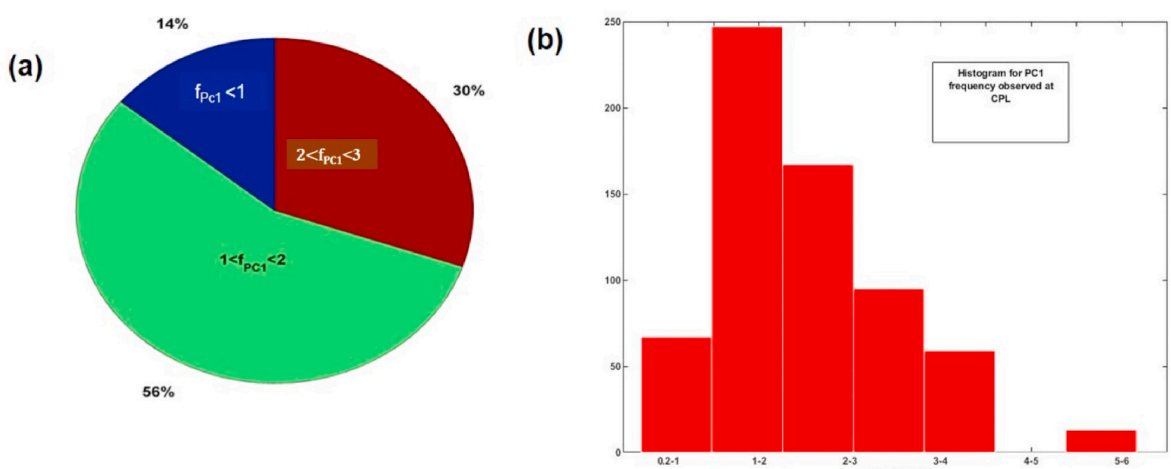

Fig. 9. (a) Distribution of Pc1 frequency and corresponding histogram in (b) at CPL.

the cycle. For example, R decreased from 220 to 95 from cycle 21 to 24. In addition, the declining phase is seen to be longer for cycles 23 and 24. The investigation throws light on the influence of these changes in the solar cycles on the occurrence patterns of Pc1 from very low and equatorial sites. The occurrence pattern, average frequency variation of Pc1 for descending phase of solar cycle 24 are shown in Fig. 11a and Fig. 11b respectively. The left ordinate (black axis) indicates the number of Pc1s and frequency of Pc1 and the right ordinate indicates the sunspot number in panels (a) and (b). The occurrence of Pc1 with sunspot number shows a similarity in trend with a lag of about a year. The number of Pc1 are minimum during 2017–18 that marks the minimum activity conditions. The comparison of average Pc1 frequency with sunspot number shows that initially the Pc1 frequency shows an increase with increasing sunspot number till 2014, the solar maximum year of cycle 24 and then decreases with decreasing sunspot number till 2016. In 2017, there is a significant increase in Pc1 frequency when the sunspot numbers dropped drastically. The average frequency of Pc1s show a direct relation with sunspot numbers at DSP (panel b, correlation coefficient is 0.4568). We looked for the variation in the minimum, maximum, median and mode frequency of Pc1with sunspot number (shown in years in panel's c and f). It should be noted that observations at DSP are for the descending phase of solar cycle 24 where the sunspots decreased from 113.3 in year 2014 (solar maximum) to 7 in 2018 (solar minimum). The mode and median frequencies show an increase in the descending phase of the solar cycle 24 at DSP (panel c). The minimum frequency remained at 0.2 Hz throughout the descending phase of cycle

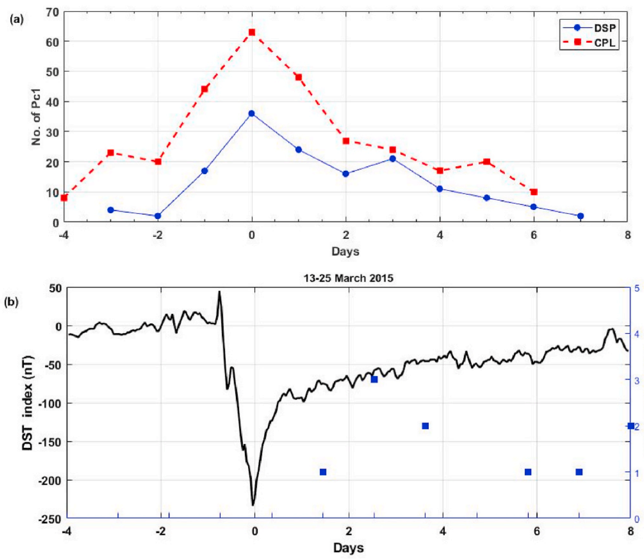

Fig. 10. (a) Superposed epoch analysis of Pc1 events with respect to geomagnetic storms in relation to |Dst| > 50 nT. The zero day on the horizontal axis corresponds to the day of main phase of geomagnetic storm; the vertical axis shows the total number of pulsations recorded during a given day. (b) Typical example of Pc1 occurrence around an intense storm during 17–23 March 2015.

24. The maximum frequency is observed at 3 Hz during the solar maximum year 2014 and decreased to 1.1 Hz in the solar minimum year 2018.

The occurrence pattern, average frequency variation of Pc1 for descending phase of solar cycle 20 to ascending phase of solar cycle 21 is shown in Fig. 11d and e respectively. The left ordinate (black axis) indicates the number of Pc1s and frequency of Pc1 and the right ordinate indicates the sunspot number in panels (d) and (e). A clear anti-correlation is seen in the number of Pc1 occurrence at CPL (panel d) (correlation coefficient is −0.3658 for CPL). The average frequency of Pc1 (shown in blue curve) initially shows an inverse relation for the descending phase of solar cycle 20 but increases with increasing sunspot number in the ascending phase of solar cycle 21 (panel e, correlation coefficient 0.6589). At CPL, the data analyzed covers part of 2 solar cycle, descending phase of solar cycle 20 (solar maximum year 1970 and minimum year 1976) and ascending phase of solar cycle 21 (solar maximum year 1980, year 1976 and 1980 marked as solar maximum). The minimum frequency showed a variation with solar cycle but remained well below 1 Hz throughout the two solar cycles. The maximum frequency reached to 3 Hz in 1972, which marked the start of descending phase of cycle 21 and remained below 2 Hz for the remaining period. It should be noted that the statistical analysis would be affected due to some gaps in the data which is shown below and also included in the appendix section.

8. Modeling of Pc1 wave propagation along the ionosphere

To evaluate the contribution of the ionosphere to the Pc1 activity, we have considered the model of the ionospheric wave propagation. We use the same numerical model of the magnetosphere - ionosphere - atmosphere - ground system as in Fedorov et al. (2016) to describe the transmission/propagation of incident EMIC waves from the magnetosphere through an inhomogeneous ionosphere to the ground. The medium is assumed to be homogeneous in the horizontal direction, i.e. along x and y. The wave modification upon propagation from the magnetosphere to the ground is determined from the solution of full wave equations with account of finite frequency terms $\sim\omega/\Omega$ in a

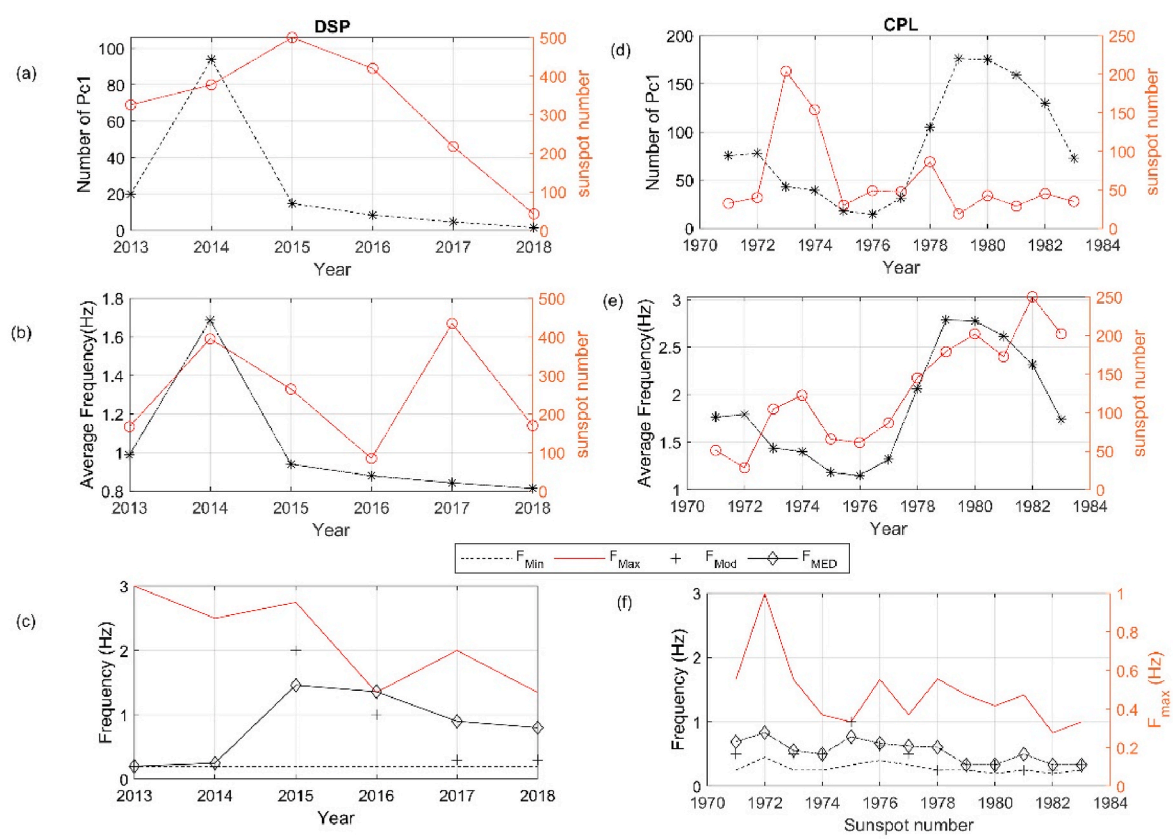

Fig. 11. Solar cycle variation of Pc1 occurrence and frequency of Pc1 in solar cycle 24 at DSP (a) (b and c) and in solar cycle 20–21 at CPL (d, e, and f). F_{min}, F_{max}, F_{Mod} and F_{Med} denote the minimum, maximum, mode and Median frequency observed for a given year.

medium with the complex permittivity tensor.

This is a numerical model that uses multi fluid magnetohydrodynamic model to provide full wave solution of magnetospheric Alfven wave and its propagation in the ionosphere. To reconstruct the altitude profile of the complex permittivity tensor elements the International Reference Ionosphere (IRI-2007) model has been used. This empirical model provides height profiles of ionospheric constituents in the altitude range from 60 km up to the ionosphere-magnetosphere interface 2000 km for any specified date and location The MHD modes are coupled owing to the frequency-dependent Hall conductivity and geomagnetic field line inclination. Invoked IRI- model uses height profiles of electron density, Ne, electron temperature Te, ion composition (O^+, N^+, H^+, He^+, O, and NO^+), ion density Ni, and ion Ti temperatures in the altitude range from 60 km up to the ionosphere-magnetosphere interface H = 2000 km with cadence of 1 km for a specified date and location. This model incorporates the COSPAR International Reference Atmosphere (1986) neutral temperature model and International Geomagnetic Reference Field model. In addition, the Mass Spectrometer Incoherent Scatter (MSIS) model has been used to obtain the altitude profiles of temperatures Tn and concentrations of neutral particles (He, O, N_2, O_2, Ar, H, and N).

The transverse structure of an incident wave packet is modeled as a beam localized in latitudinal direction, whereas the beam azimuthal structure is assumed to be a plane wave with a finite azimuthal wave scale ky = $1.7 \cdot 10^{-3}$ km^{-1}. Though the magnitude of ground response and the decay rate upon propagation away from an incidence region depend on the wave beam parameters, the spatial structure on ground is to be qualitatively similar. The ground Pc1 wave structure produced by an incident magnetospheric wave beam has been calculated for the source located at geomagnetic latitude 62° (L = 4.6). This latitude corresponds to typical location of the driving EMIC instability. The results of the model may be qualitatively applied to any mid-latitude and low-latitude observation site. We do not have specific data about the ionospheric parameters during recorded Pc1 events, therefore the results just qualitatively describe the contrast between day/night propagation towards equator for various frequencies.

Fig. 12 shows the spatial distribution of amplitudes of horizontal magnetic component $|B_x(x)|$ along latitude (expressed in km from the incidence of wave). In the vicinity of the incidence region, $|x|<300$ km, the latitudinal structure of $B_x(x)$ on the ground “duplicates” qualitatively the spatial structure of incident Alfven beam.

The observations discussed above were performed far away from a probable Pc1 source, therefore the main effect of the ionosphere is the control of the distant wave propagation along the Earth’s surface. The wave spreading along the ground at large distances is a leakage of wave energy from an incidence region by propagating waveguide modes. The

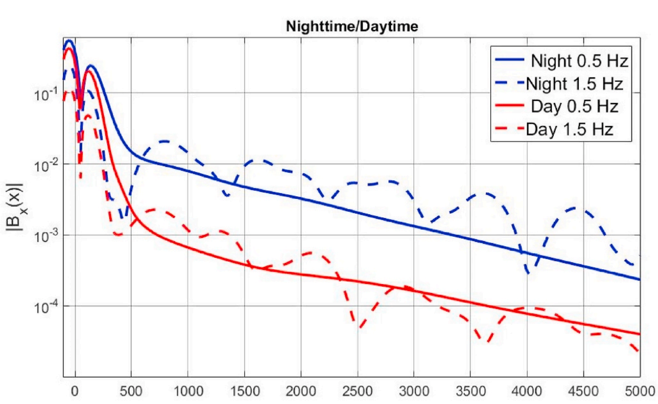

Fig. 12. The latitudinal distribution of amplitudes of horizontal magnetic component $|B_x(x)|$ for dayside (red lines) and nighttime (blue lines) ionospheres. We suppose that the amplitude of the incident wave is 1 nT.

modeling demonstrates an inhomogeneous decay of wave amplitude. The largest decay rate is observed near the ground image of the incident wave beam. At distances >400 km, the main contribution to the ground magnetic response is produced by waveguide modes. The waveguide critical frequency can be estimated as $f_c = V_A/d \propto 1/\sqrt{N_e}$, where V_A and *N*e are the Alfven velocity and plasma density of the ionospheric F-layer, d is the vertical scale of the ionospheric waveguide. Waves with $f < fc$ cannot be trapped in the waveguide, and decay exponentially with distance. During the daytime, when *N*e is higher, fc is lower than during the nighttime.

As evident from Fig. 12, waveguide mode with $f = 0.5$ Hz day gradually upon distance from a source, during both daytime and nighttime. Comparison of daytime and nighttime conditions shows that at large distances from a source the amplitude of ground response at nighttime is nearly order of magnitude larger than during daytime. For higher frequencies, >1 Hz, excitation of more than one waveguide modes becomes possible. In this case a nonmonotonic spatial pattern forms because of the interference between waveguide modes. During nighttime wave modes with higher frequencies (e.g., 1.5 Hz) trapped in the ionospheric waveguide propagate more effectively than modes with lower frequencies. Thus, even the simplified model demonstrates that lower ionospheric density favors the Pc1 wave propagation to large distances equatorward. This conjecture is in accordance with diurnal and solar cycle variations of Pc1 wave occurrence with various frequencies, presented above.

9. Discussion

There have been many previous studies that provides the Pc1 properties in the middle and high latitudes. The investigation presented in this work is unique which provides insights to the very low latitude regions. In this study, we elucidate on the morphology, diurnal, seasonal, storm time Pc1, solar cycle and propagation of Pc1 events to low and equatorial region from Indian region during different solar cycles. The diurnal pattern and relation of Pc1 to geomagnetic storms are similar at both stations. The seasonal dependence looks different at the two sites which may be due to unevenness of data lengths at both sites (data availability is included in the supporting file). Nevertheless, solar cycle variations indicate a clear inverse relation between sunspot number and Pc1 occurrence at both DSP and CPL. While we demonstrate the similar characteristics of Pc1s as observed at high and mid latitudes, we also attempt to provide a unique propagation model of Pc1s to the lower latitudes.

The observational results indicate that the ionospheric plasma density is a critical factor that determines the occurrence of Pc1 waves at near-equatorial latitudes. The physical reason is that the attenuation of Pc1 waves upon propagation via the ionospheric waveguide towards lower latitudes is weaker during night hours. Similarly, during the period of solar maximum the transmission rate of Pc1 waves to the equator may be diminished than during the solar minimum. This fact may explain, at least partly, the anticorrelation between the Pc1 wave occurrence at very low latitudes and solar activity. In line with these features, the diurnal occurrence pattern shows a maximum in the pre-midnight and post-midnight hours, whereas minimum number of Pc1 are seen during local noon and post noon hours.

Our observational results are in accordance with observations at other latitudes. Mursula et al. (1991) analyzed the sub-auroral magnetograms over the period covering nearly four solar cycles. The results showed a strong negative correlation between the Pc1 activity and the annual sunspot number which persisted over the whole data period. At low-latitude station (geomagnetic latitude ~34.4°) during one solar cycle Fujita and Owada (1986) found that Pc1 pulsations appeared mainly in nighttime, in winter, and in the period of the minimum solar activity. However, Kawamura et al. (1983) found no distinctive seasonal and annual variations in occurrence of Pc1 emissions at sub-auroral

Syowa station. This difference between statistical occurrences at various latitudes can be attributed to the different combination of such factors as the generation, magnetospheric field-aligned propagation, and ionospheric spreading of Pc1 waves.

To comprehend basic properties of the Pc1 wave transmission from middle towards very low latitudes, we have used the numerical model that provides full wave solution of magnetospheric Alfven wave beam propagation through the ionosphere to the ground, and its partial conversion into the ionospheric waveguide modes. The modeling describes the wave propagation pattern qualitatively because of simplicity of the source as azimuthally large-scale wave. According to the model, during nighttime hours the magnetic intensity at distance $\sim 5 \cdot 10^3$ km drops about 2–3 orders of magnitude as compared with a source region, but the modeled damping rates hardly can be applied to actual observations. Nonetheless, the predicted dependence of the propagation properties on the ionospheric density is trustworthy. The modeling confirms that low-density ionospheric conditions and higher wave frequencies favors the Pc1 pulsation transmission towards near-equatorial latitudes.

10. Conclusion

Multi-year induction coil magnetometer observation covering digital and archived magnetometer records over different solar cycles at Indian sub-continent bring out interesting results. Digital records, covering the solar maximum and descending phase of solar cycle 24, from DSP showed that Pc1s populate in the post and pre-midnight sector. Similar diurnal patterns is observed in the archived magnetometer records from CPL that covered solar cycle 20 and 21. A clear anti correlation is observed between the solar cycle and Pc1 occurrence pattern. Similar diurnal and solar cycle dependence is earlier reported at high latitude station Mursula et al. (1991) and low latitude stations Fujita and Owada (1986). Investigation of Pc1 occurrence in relation to geomagnetic storm showed similar characterises at both the stations and also the results are consistent with observation from other latitudes. Maximum number of Pc1s are seen during the recovery phase of the storm, followed by the storm main phase. This is consistent with observation of Bortnik et al. (2008).

Apart from the Pc1 trends over various temporal scales observed from the magnetometer records we also provide a model to address the effective propagation of Pc1s along the ionosphere down to the geomagnetic equator. Penetration of Pc1 waves towards the near-equatorial latitudes during nighttime turned out to be more efficient than during near-noon hours. During nighttime, Pc1 waves statistically can reach the equator with frequencies in a range 0.2–3.0 Hz, whereas during daytime fewer number of recorded Pc1 waves had frequencies >0.5 Hz. The modeling confirms that the waveguide mode attenuation is larger in the daytime ionosphere than that in the nighttime ionosphere, and the decay rate of waveguide modes with higher frequencies is to be weaker.

Declaration of competing interest

The authors declare that they have no known competing financial interests or personal relationships that could have appeared to influence the work reported in this paper.

Data availability

Data will be made available on request.

Acknowledgements

This work has been carried out under the research collaboration of CSIR-NGRI, Hyderabad and ISR, Gujarat. This is CSIR-NGRI contribution NGRI/Lib/2021/Pub-70. JB thanks DST-INSPIRE Faculty for the support provided to carry out the research work.

Appendix A

The availability of complete Digital and archived records are shown in Fig. A1. It should be noted that the months for which data was either noisy or was not available for more than 15 days are not considered for investigation in this study. Top panel denotes the available digital data from DSP and bottom panel denotes the archived data availability. It is seen that the data in the year 2017 and 2018 are sparse. This could have resulted in the observed seasonal pattern at DSP.

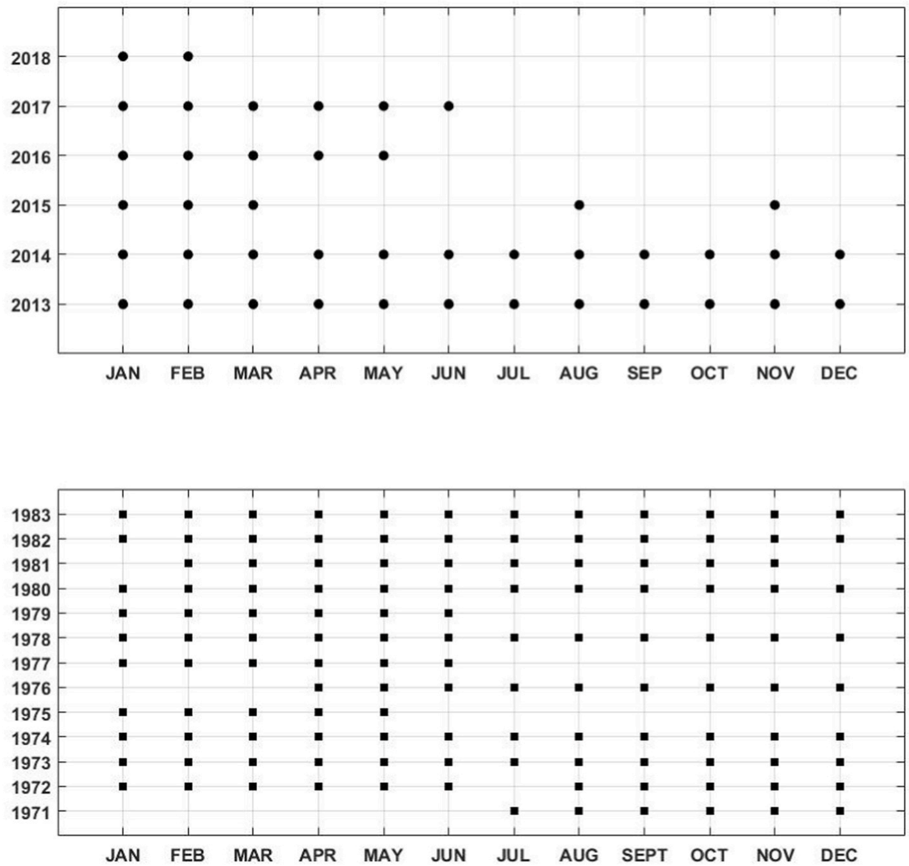

Fig. A1. Availability of digital data at DSP (top) and archived charts at CPL (bottom) used in this study.

References

Anisimov, S.V., Shikhova, N.M., Kleimenova, N.G., 2018. Midlatitude *Pc*1 geomagnetic pulsations: results of observations and statistical estimates. Izvestiya Phys. Solid Earth 54, 688–697. https://doi.org/10.1134/S1069351318050026.

Engebretson, M.J., Moen, J., Posch, J.L., Lu, F., Lessard, M.R., Kim, H., Lorentzen, D.A.(, 2009. Searching for ULF signatures of the cusp: observations from search coil magnetometers and auroral imagers in Svalbard. J. Geophys. Res. 114, A06217 https://doi.org/10.1029/2009JA014278.

Bortnik, J, Cutler, J.W., Dunson, C, Bleier, T.E., McPherron, R.L., 2008. Characteristics of low-latitude Pc1 pulsations duringgeomagnetic storms. J. Geophys. Res. 113 https://doi.org/10.1029/2007JA012867.

Bulusu, Jayashree, Kusumita, Arora, Nandini, Nagarajan, 2017. Detailed study of Pi2 damped oscillations from low latitude magnetic observatory. J. Atmos. Sol. Terr. Phys. 155, 12–21.

Engebretson, M.J., Kahlstorf, C.R.G., Murr, D.L., Posch, J.L., Keiling, A., Lavraud, B., Rème, H., Lessard, M.R., Kim, E.-H., Johnson, J.R., Dombeck, J., Grison, B., Robert, P., Glassmeier, K.-H., Décréau, P.M.E., 2012. Cluster observations of band-limited Pc 1 waves associated with streaming H+ and O+ ions in the high-altitude plasma mantle. J. Geophys. Res. 117, A10219 https://doi.org/10.1029/2012JA017982.

Fedorov, E., Mazur, N., Pilipenko, V., Engebretson, M., 2016. Interaction of magnetospheric Alfven waves with the ionosphere in the Pc1 frequency band. J. Geophys. Res. 121, 321–337.

Fraser, B.J., Loto'Aniu, T.M., Singer, H.J., 2006. Electromagnetic ion cyclotron waves in the magnetosphere. In: Takahashi, K., Chi, P.J., Denton, R.E., Lysak, R.L. (Eds.), Magnetospheric ULF Waves: Synthesis and New Directions", Washington DC, AGU Geophysical Monograph Series, vol. 169, p. 195.

Fraser, B.J., Singer, H.J., Hughes, W.J., Wygant, J.R., Anderson, R.R., Hu, Y.D.(, 1996. CRRES Poynting vector observations of electromagnetic ion cyclotron waves near the plasmapause. J. Geophys. Res. 101, 15331–15343. https://doi.org/10.1029/95JA03480.

Fujita, S., Owada, T., 1986. Occurrence characteristics of Pc1 pulsations observed at Japanese observatory network. Mem. Natl. Inst. Polar Res. 42, 79–91.

Greifinger, C., Greifinger, P., 1973. Wave guide propagation of micropulsations out of the plane of the geomagnetic meridian. J. Geophys. Res. 78, 4611–4618.

Guglielmi, A., Potapov, A., Matveyeva, E., Polyushkina, T., Kangas, J., 2006. Temporal and spatial characteristics of Pc1 geomagnetic pulsations. Adv. Space Res. 38, 1572–1575.

Hayashi, K., Kokubun, S., Oguti, T., Tsuruda, K., Machida, S., Kitamura, T., Saka, O., Watanabe, T., 1981. The extent of Pc 1 source region in high latitudes. Can. J. Phys. 59, 1097–1105.

Kangas, J., Guglielmi, A., Pokhotelov, O., 1998. Morphology and physics of short-period geomagnetic pulsations. Space Sci. Rev. 83, 435–512. https://doi.org/10.1023/A:1005063911643.

Kennel, C.F., Petchek, H.E., 1966. Limit on stably trapped particle fluxes. J. Geophys. Res. 71 (N1), 1–28.

Kawamura, M., Kuwashima, M., Toya, T., Fukunishi, H., 1983. Comparative study of magnetic Pc1 pulsations observed at low and high latitudes: long term variation of occurrence frequency of the pulsations. Mem. Natl. Inst. Polar Res. - Special Issue 26, 1–12.

Kim, Jiwoo, et al., 2020. Statistical Analysis of Pc1 Pulsations Observed by a BOH Magnetometer. J. Astron. Space Sci. 37 https://doi.org/10.5140/JASS.2020.37.1.19.

Kim, H., Lessard, M.R., Engebretson, M.J., Luhr, H., 2010. Ducting characteristics of Pc 1 waves at high latitudes on the ground and in space. J. Geophys. Res. 115, 310. https://doi.org/10.1029/2010JA015323. A09.

Kim, H., Lessard, M.R., Engebretson, M.J., Young, M.A., 2011. Statistical study of Pc1-2 wave propagation characteristics in the high-latitude ionospheric waveguide. J. Geophys. Res. 116, 227. https://doi.org/10.1029/2010JA016355.

Kuwashima, M., Toya, T., Kawamura, M., Hirasawa, T., Fukunishi, H., Ayukawa, M., 1981. Comparative Study of Magnetic Pc1 Pulsations between Low Latitudes and High Latitudes: Statistical Study, vol. 18. National Institute Polar Research Memoirs, pp. 101–117.

Lee, D.-H., Johnson, J.R., Kim, K., Kim, K.-S., 2008. Effects of heavy ions on ULF wave resonances near the equatorial region. J. Geophys. Res. 113, A11212 https://doi.org/10.1029/2008JA013088.

Mursula, K., Kangas, J., Pikkarainen, T., Kivinen, M., 1991. Pc 1 micropulsations at a high-latitude station: a study over nearly four solar cycles. J. Geophys. Res. 96 (A10), 17651–17661. https://doi.org/10.1029/91JA01374.

Nomura, R., Shiokawa, K., Pilipenko, V., Shevtsov, B., 2011. Frequency-dependent polarization characteristics of Pc1 geomagnetic pulsations observed by multipoint ground stations at low latitudes. J. Geophys. Res. 116, A01204 https://doi.org/10.1029/2010JA015684.

Park, J., Lühr, H., Rauberg, J., 2013. Global characteristics of *Pc*1 magnetic pulsations during solar cycle 23 deduced from CHAMP data. Ann. Geophys. 31, 1507–1520.

Pickett, J.S., Grison, B., Omura, Y., Engebretson, M.J., Dandouras, I., Masson, A., Adrian, M.L., Santolík, O., Décréau, P.M.E., Cornilleau-Wehrlin, N., Constantinescu, D., 2010. Cluster observations of EMIC triggered emissions in association with Pc1 waves near Earth's plasmapause. Geophys. Res. Lett. 37, L09104 https://doi.org/10.1029/2010GL042648.

Pilipenko, V.A., Chugunova, O.M., Engebretson, M.J., Lessard, M., 2011. Trans-polar propagation of Pi1 wave burst as observed by an antarctic array during the themis 2007/03/23 substorm, "physics of auroral phenomena". In: Proc. 34 Annual Seminar, pp. 86–89. Apatity.

Posch, J.L., Engebretson, M.J., Murphy, M.T., Denton, M.H., Lessard, M.R., Horne, R.B., 2010. Probing the relationship between electromagnetic ion cyclotron waves and plasma spheric plumes near geosynchronous orbit. J. Geophys. Res. 115, A11205 https://doi.org/10.1029/2010JA015446.

Sarma, Y.S., Sanker Narayan, P.V., Ramanujachary, K.R., Sarma, S.V.S., 1969. Three component induction magnetometer for recording geomagnetic micropulsations at the geoelectric observatory at Choutuppal. Bull. Ngri. 7 (1), 51.

Sastry, T.S., Sarma, Y.S., Sarma, S.V.S., 1983. Daytime Pi pulsations at equatorial latitudes. J. Atmos. Terr. Phys. 45, 733.

Sastry, T.S., S Sarma, Y., S Sarma, S.V., Sanker Narayan, P.V., 1978. A study of pearl pulsations in the equatorial region of India. J. Atmos. Terr. Phys. 40, 1289–1296. https://doi.org/10.1016/0021-9169(78)90080-6.

Shprits, Y.Y., Drozdov, A.Y., Spasojevic, M., Kellerman, A.C., Usanova, M.E., Engebretson, M.J., Agapitov, O.V., Zhelavskaya, I.S., Raita, T.J., Spence, H.E., Baker, D.N., Zhu, H., Aseev, N.A., 2016. Wave-induced loss of ultra-relativistic electrons in the Van Allen radiation belts. Nat. Commun. 7, 12883 https://doi.org/10.1038/ncomms12883.

Sinha, Ashwini Kumar, Pathan, B M, Vohat, P, 2007. Low latitude Pc1 pulsation as observed from ground-based search coil magnetometer. Bull. Astr. Soc. India 35, 533–538.

Trakhtengerts, V.Y., Demekhov, A.C., Belyaev, P.P., Polyakov, S.V., Ermakova, E.N., Isaev, S.V., 2000. A mechanism of anticorrelation in the occurrence of ULF electromagnetic noise resonance structure and Pc1 magnetic pulsations through the solar activity cycle. J. Atmos. Solar-Terr. Phys. 62, 253–256.

Usanova, M.E., Drozdov, A., Orlova, K., Mann, I.R., Shprits, Y., Robertson, M.T., Turner, D.L., Milling, D.K., Kale, A., Baker, D.N., Thaller, S.A., Reeves, G.D., Spence, H.E., Kletzing, C., Wygant, J., 2014. Effect of EMIC waves on relativistic and ultra-relativistic electron populations: ground-based and Van Allen Probes observations. Geophys. Res. Lett. 41, 1375–1381. https://doi.org/10.1002/2013GL059024.

Webster, D.J., Fraser, B.J., 1984. Source structure and dynamics of Pc1 pulsations at low latitudes. Planet. Space Sci. 32, 935–947.

Webster, D.J., Fraser, B.J., 1985. Source regions of low-latitude Pc1 pulsations and their relationship to the plasmapause. Planet. Space Sci. 33 (7), 777–793. https://doi.org/10.1016/0032-0633(85)90032-7.

Yahnin, A.G., Yahnina, T.A., Frey, H.U., 2007. Subauroral proton spots visualize the Pc1 source. J. Geophys. Res. 112, A10223 https://doi.org/10.1029/2007JA012501.